Estimation of undrained behavior of sand from self-boring pressuremeter tests

Estimation du comportement d'un sable non drainé à l'aide de tests pressiométriques

Debasis Roy, R.G.Campanella & Peter M. Byrne – *Department of Civil Engineering, University of British Columbia, Vancouver, B.C., Canada*

J.M.O. Hughes – *Hughes In-Situ Engineering, Inc., Vancouver, B.C., Canada*

ABSTRACT: An analytical procedure for estimation of undrained behavior of sand using self-boring pressuremeter data has been proposed. Data from two sites have been analyzed following the procedure to predict the mechanical behavior of axially symmetric elements. For validation of the procedure the predicted axisymmetric response was compared with the triaxial test data on undisturbed (frozen) samples.

RÉSUMÉ: Une procédure analytique a été proposée pour estimer le comportement d'un sable non drainé utilisant les données recueillis à l'aide d'un pressiomètre auto-foureur. Des données provenant de deux sites ont été analysées suivant cette procédure afin d'estimer le comportement mécanique d'éléments axi-symétriques. Pour vérifier la procédure proposée, ces résultats axi-symétriques furent comparés aux résultats d'essais triaxiaux effectués sur des échantillons non-pertubés (gelés).

1 INTRODUCTION

Empirical procedures have been proposed for obtaining undrained strength of cohesionless materials from index tests, e.g., Piezocone Penetration Test (CPTU) and Standard Penetration Test or SPT (e.g., Stark and Mesri, 1992). However a majority of the correlations upon which these procedures are based are rather imprecise. Consequently, the success of these procedures have been limited. A procedure for estimating the undrained monotonic response of sand is proposed here based on inverse modeling of self-boring pressuremeter tests (SBPMT). An elastoplastic stress-strain model is used in the analyses. To illustrate the proposed procedure, an estimate of model parameters has been derived from SBPMTs at two sites. Axisymmetric element response is then computed from these parameters. The results are compared with the triaxial test data on undisturbed sample from the same sites to validate the procedure.

2 MODELING ELASTIC STRESS-STRAIN BEHAVIOR

For isotropic elastic material, the strain increment is given by

$$d\epsilon_{ij}^{\,e} = D_{ijkl}^{\,e}\, d\sigma_{kl}' = (C_{ijkl}^{\,e})^{-1}\, d\sigma_{kl}' \qquad (1)$$

where σ_{kl}' is the effective Cauchy stress and $D_{ijkl}^{\,e}$ is the elastic compliance tensor. The elastic stiffness tensor, $C_{ijkl}^{\,e}$, is given by

$$C_{ijkl}^{\,e} = \frac{2E}{1+\nu}\left(\frac{2\nu}{1+2\nu}\delta_{ij}\delta_{kl} + \delta_{ik}\delta_{jl} + \delta_{il}\delta_{jk} + \frac{2\xi(1+\nu)}{1-\xi}\frac{\sigma_{ij}'\sigma_{kl}}{\sigma_e'^{2}} \right) \qquad (2)$$

where δ_{ij} represents Kronecker delta, $\xi = \sigma_e'\{dE/d\sigma_e'\}/E$ and $\sigma_e' = [(1-2\nu)\sigma_{kk}'^{2}/3 + 2(1+\nu)J_2]^{0.5}$. The Poisson's ratio, ν, is a model parameter. The secant Young's modulus, E, for a hyperelastic material can be expressed as (Lade and Nelson, 1987)

$$E = K_E P_A \left[\left(\frac{I_1}{P_A} \right)^2 + 6\frac{1+\nu}{1-2\nu}\frac{J_2}{P_A^{\,2}} \right]^{n_E} \qquad (3)$$

where K_E (the elastic Young's modulus number), n_E (elastic exponent) are model parameters and P_A is the atmospheric pressure. The invariants I_1 and J_2 are given by

$$I_1 = \sigma_{ii}',\ J_2 = I_1^2 - 3I_2,\ \text{where } I_2 = \{(\sigma_{kk}')^2 - \sigma_{ij}'\sigma_{ij}'\}/2 \qquad (4)$$

The value of the exponent n_E varies over a very narrow range of 0.23 to 0.26 for a number of sands. A value of 0.2 can be assumed for the Poisson's Ratio for many sands irrespective of the void ratio. Parameter K_E mainly depends on soil type and the state of packing. The appropriate in-situ estimate of K_E can be found from shear wave velocity measurements from seismic CPTU and a reasonable knowledge of in-situ state of stress for young uncemented sand. To account for the influence of the state of packing on E, the value of K_E is updated during the deformation process in proportion with $(2.17-e)^2/(1+e)$. Typical values of some of the model parameters can be found in Table 1. Values for many other soils have been given by Lade and Nelson (1987).

Table 1. Elastic Model Parameters

Sand type	D_R, %	K_E	n_E
Fraser	38	883	0.25
River	50	1100	0.25
Syncrude	65	740	0.25
	43	390	0.25

3 MODELING IRREVERSIBLE DEFORMATION

The irreversible behavior in distortion is often modeled by adopting a loading surface that has an appearance similar to a cone in the principal stress space with its apex at the origin. Since the conical loading surface opens out along the hydrostatic axis, the distortion mechanism does not predict irreversible deformation in isotropic compression. Such a deformation is usually much smaller than that in a distortional loading. However, since in the problem of our interest - cylindrical cavity expansion - the mean effective stress may increase significantly, the irreversible deformation due to isotropic loading needs to be accounted for. Towards this, a second loading surface is introduced. For isotropic materials, the loading surface for isotropic compression takes a spherical shape in the principal effective stress space and is sometimes called the "cap". The plasticity mechanisms for

distortion and isotropic compression are assumed to be mutually non-interactive and of the strain hardening type.

3.1 *A Model for Distortional Behavior of Isotropic Materials*

The Spatial Mobilized Plane (SMP) is defined in such a manner that at the intersection of this plane and the plane normal to the principal direction "k" of the effective stress tensor, the ratio, $(\sigma_{(i)}'-\sigma_{(j)}')/(\sigma_{(i)}'+\sigma_{(j)}')$, is maximized (Nakai and Matsuoka, 1983). The direction cosines, a_i, of a unit normal to the SMP with respect to the principal directions are given by

$$a_i = \sqrt{I_3 / (I_2 \sigma_{(i)}')} \tag{5}$$

where $\sigma_{(i)}'$ are the principal values of σ_{ij}'. The third invariant of the effective stress tensor, I_3, is equal to the determinant of σ_{ij}'. The normal (σ_{SMP}) and the shear (τ_{SMP}) components of the effective stress tensor on this plane and the ratio σ_{SMP} to τ_{SMP}, η (often referred to as the stress ratio), are given by

$$\sigma_{SMP} = 3 I_3 / I_2, \quad \tau_{SMP} = \sqrt{I_1 I_3 / I_2 - 9 I_3^2 / I_2^2}$$
$$\eta = \sqrt{I_1 I_2 / (9 I_3) - 1} \tag{6}$$

Constant η lines represent the loading surfaces, i.e., yielding occurs when $\partial\eta/\partial\sigma_{ij}' d\sigma_{ij}' \geq 0$. Assuming the particles are mobilized to the maximum extent on the average along the SMP, it follows from micro mechanical considerations that

$$\eta = -\lambda (d\epsilon_{SMP} / d\gamma_{SMP}) + \mu \tag{7}$$

where $d\epsilon_{SMP}$ and $d\gamma_{SMP}$ are the components of $d\epsilon_{(i)}^{*}$ normal and parallel to the SMP. $d\epsilon_{(i)}^{*}$, denotes the principal values of the strain increment of the mechanism for distortional plasticity, $d\epsilon_{ij}^{*}$. λ and μ are model parameters. Assuming a hyperbolic relationship between γ_{SMP} and η the instantaneous slope, G_{PT} (= $d\eta/d\gamma_{SMP}$), can be calculated from (Salgado, 1990)

$$G_{PT} = G_{PI} (1 - R_F \eta / \eta_F)^2$$
$$= K_{SP} (\sigma_{SMP} / P_A)^{n_P} (1 - R_F \eta / \eta_F)^2 \tag{8}$$

where G_{PI} is the initial slope of the η-γ_{SMP} curve, η_{ULT} is the asymptotic value of stress ratio approached as γ_{SMP} increases. K_{SP}, n_P and R_F are model parameters. The stress ratio at failure, η_F, is assumed to depend on I_{1F}, the first invariant of the effective stress tensor at failure, as follows

$$\eta_F = \eta_{F1} - \Delta\eta \log \{ I_{1F} / (3 P_A) \} \tag{9}$$

where η_{F1} and $\Delta\eta$ are model parameters. From Eqs. (7) and (8)

$$d\epsilon_{SMP} = (\mu - \eta) / (\lambda G_{PT}) \, d\eta \tag{10}$$

Assuming the principal directions of $d\epsilon_{ij}^{*}$ and σ_{ij}' to be the same, the direction cosines of $d\epsilon_{SMP}$ can be calculated from Eq. (5). Assuming further that $d\gamma_{SMP}$ and τ_{SMP} are coaxial, $d\epsilon_{(i)}^{*}$ can be calculated from

$$d\epsilon_{(i)}^{*} = a_i \{ d\epsilon_{SMP} + d\gamma_{SMP} (\sigma_i' - \sigma_{SMP}) / \tau_{SMP} \}$$
$$= a_i / G_{PT} \{ (\mu - \eta)/\lambda + (\sigma_i' - \sigma_{SMP}) / \tau_{SMP} \} \, d\eta \tag{11}$$

Differentiating η from Eq. (6) and substituting into Eq. (11), an incremental relationship between the principal strain and the effective stresses is obtained. Transformation of the strain increment tensor in the principal stress space, $d\bar{\epsilon}_{ij}^{*}$ (= $d\epsilon_{(i)}^{*} \delta_{ij}$), to the coordinate axes using $d\epsilon_{ij}^{*} = N_{ik} N_{jl} d\bar{\epsilon}_{ij}^{*}$ yields

$$d\epsilon_{ij}^{e} = D_{ijkl}^{*} \, d\sigma_{kl}' \tag{12}$$

where N_{ij} represents the direction cosine of the principal direction "i" with respect to the j-th coordinate.

3.2 *Modeling Inherent Anisotropy*

The model parameters λ and μ are not affected by the inherent anisotropy (Nakai and Matsuoka, 1983). Studies also suggest that the quantity η_F may not be significantly affected by inherent anisotropy (see, e.g., Been and Jefferies, 1985). Thus, Eq. (8) only needs to be modified to capture inherent anisotropy. Following modification to Eq. (8) is used in this study

$$G_{PT} = G_{PI} (1 - R_F \eta / \eta_F)^2$$
$$= n_A K_{SP} (\sigma_{SMP} / P_A)^{n_P} (1 - R_F \eta / \eta_F)^2 \tag{13}$$

where the multiplier n_A depends on θ (the angle between the depositional direction and the normal to the SMP) and an additional model parameter, m_A, as follows for $0^0 \leq \theta \leq 45^0$ (for $\theta \leq 45^0$, $n_A = 1$)

$$n_A = 1 - (m_A - 1)(2\cos^2\theta - 1) \tag{14}$$

In computation the variation in G_{PT} due to the change in the value of θ is neglected over a single time step. This assumption may not lead to a significant error for small time steps.

3.3 *Modeling Irreversible Deformation in Isotropic Compression*

To evaluate the component of plastic strain, $d\epsilon_{ij}^{c}$, due to isotropic compression, an associated plasticity model proposed by Lade (1977) for isotropic materials is used. The loading surface for this formulation is given by

$$f_C = I_1^2 - 2 I_2 = \sigma_{ij}' \sigma_{ij}' \tag{15}$$

The relationship essentially represents a family of spherical surfaces in the effective principal stress space. Section of the loading surfaces for the distortion (AOB) and consolidation mechanisms (AB) in triaxial plane are shown schematically in Figure 1. Abbreviations "TXC" and "TXE" are used to denote triaxial compression and extension, respectively. It can be shown that the plastic strain increment, $d\epsilon_{ij}^{c}$, can be found from

$$d\epsilon_{ij}^{c} = \frac{C p}{2 f_C P_A} \left(\frac{f_C}{P_A^2} \right)^{p-1} \frac{\partial f_C}{\partial \sigma_{ij}'} \frac{\partial f_C}{\partial \sigma_{kl}'} \, d\sigma_{kl}' \tag{16}$$

Eqs. (1), (12), (16) are added together to calculate the total strain increment.

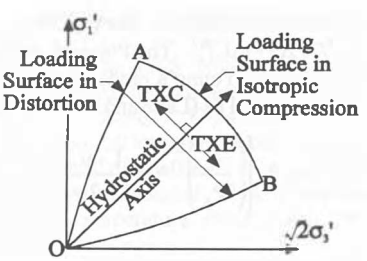

Figure 1. Loading Surfaces

3.4 *Plastic Model Parameters*

Two triaxial compression, one triaxial extension, and two isotropic compression on undisturbed samples are needed for an adequate characterization of a granular deposit at a certain depth. Such an elaborate laboratory testing program is seldom feasible. Available information often include data from undrained laboratory element tests on undisturbed samples or in-situ self-boring pressuremeter tests, which are not conventionally used in calibration of constitutive models. Although such data may not provide necessary and sufficient information for model calibration, they can nevertheless be used if reasonably precise information about the bounds of values of the model parameters is available. Existing information on the approximate values of the plastic model parameters is summarized below.

Examination of isotropic consolidation tests shows that the parameter, C, is mainly affected by the relative density, D_R, and grain compressibility. The exponent, p, on the other hand, is affected primarily by grain compressibility and is rather insensitive to the state of packing. Since the model does not recognize inherent anisotropy in isotropic loading, it is not expected to capture the effect of sample fabric for a stress path aligned with the hydrostatic axis. A relationship is proposed in Figure 2 between parameter C and D_R, which can be used in the absence of more precise information. Parameter p admits a value of 0.9 for granular materials with medium compressibility, while $p \approx 0.65$ for highly compressible soils.

Guidelines for selecting approximate values of λ, μ, η_{F1}, $\Delta\eta$, R_F, n_P and m_A from a minimal material specific information are as follows. Once the approximate values of these parameters are identified, model calibration simplifies greatly because iteration over the remaining model parameter, K_{SP}, is only necessary to fit the model to data.

λ and μ: Nakai and Matsuoka (1983) showed that Eq. (7) does not depend on void ratio or sample fabric and is affected only by soil type. Hence λ and μ, can be evaluated from a suitable drained element test, e.g., triaxial or plane strain, on reconstituted specimens. Table 2 summarizes some values of λ and μ.

η_{F1} and $\Delta\eta$: In TXC, η relates to the mobilized effective stress friction angle, ϕ', by

$$\eta = 2\sqrt{2}\tan\phi'/3 \qquad (17)$$

From an examination of a large number of triaxial tests on several types of sand, Bolton (1986) proposed a correlation between (ϕ'_F-ϕ_{CV}), relative density and I_{RF}, where ϕ'_F is the peak effective stress friction angle. Values of the steady state friction angle, ϕ_{CV}, which primarily depends upon mineralogy, has been reported in the literature for many types of sand (see, e.g., Salgado, 1990; Sasitharan et al., 1994). The correlation proposed by Bolton can thus be used to estimate of η_{F1} and $\Delta\eta$ from a knowledge of D_R.

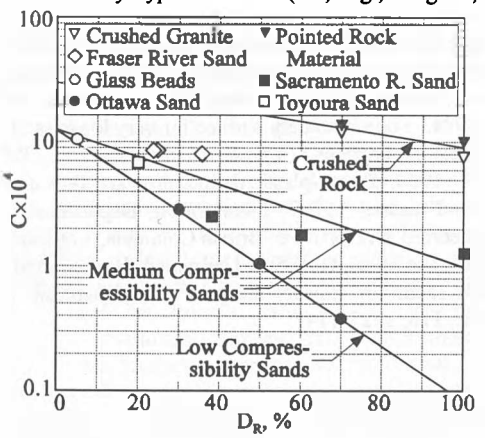

Figure 2. Parameter "C" for Dilatational Mechanism

The angle of internal friction measured in a laboratory element test allowing drainage is usually higher than the corresponding value from an undrained test. Since η relates directly to the peak friction angle in triaxial compression via Eq. (17), model parameters η_{F1} and $\Delta\eta$ are expected to be depend upon the drainage condition. Examination of a number of laboratory element test data on several sands leads to the following relationship (the square of the correlation between the two variables, $R^2 = 0.94$)

$$(\eta_F - \eta_{CV})_{Undrained} = 0.46\,(\eta_F - \eta_{CV})_{Drained} \qquad (18)$$

Table 2. λ and μ for Some Sands

Sand Type	λ	μ
Erksak	0.83	0.30
Fraser River	0.77	0.39
Hilton Mines	0.80	0.40
Ottawa C109	0.85	0.26
Syncrude	0.85	0.29
Ticino	0.87	0.33
Toyoura	0.90	0.27

The quantity, η_{CV}, is obtained using ϕ_{CV} instead of ϕ' in Eq. (17). Estimates of η_{F1} and $\Delta\eta$ pertinent to a certain drainage condition can be obtained by modifying the correlation suggested by Bolton according to Eq. (18).

R_F and n_P: R_F primarily depends on D_R. Since the parameter governs the magnitude of irreversible distortion at peak stress ratio, which in turn is not significantly affected by sample fabric and stress path, the effect of stress path and fabric on R_F is expected to be minimal. Experience with the use of a similar model (Srithar, 1994) appears to indicate that R_F admits a value of about 0.75 for very dense cohesionless soils and a value near unity for very loose deposits. In the absence of material specific information, for an approximate estimate of R_F, linear interpolation is used in this study setting R_F=1.0 at D_R=0 and R_F=0.75 at D_R=100%. Previous experience with the distortion mechanism used in this study (Salgado, 1990; Srithar, 1992) indicate that n_P ranges between -0.3 and -0.6 for many sands. In this study, a number of laboratory triaxial tests on several sands could be simulated using n_P=-0.5.

m_A: Analysis of a large number of laboratory triaxial tests on undisturbed samples indicates that a value of 2.0 is typical for deposits formed in a hydraulic deposition process such as spigotting of mine tailings or fluvial deposition of channel sands.

4 UNDRAINED ELEMENT BEHAVIOR FROM SBPMT

Two cavity expansion tests performed at Massey Tunnel (a Holocene channel deposit of Fraser River Sand) and J-Pit (a deposit spigotted Syncrude Sand) were analyzed as plane strain problem. The original effective vertical stress, σ_v', was assumed to be $2\sigma_h'$, where σ_h' is the original horizontal effective stress. For the deposit at J-Pit $D_R \approx 30\%$ while at Massey Tunnel $D_R \approx 50\%$. For J-Pit and Massey Tunnel ϕ_{cv} of 28° and 32° was assumed. These tests were conducted using a monocell self-boring pressuremeter with a length to diameter ratio of about 6. A finite difference computer code (FLAC version 3.2, Cundall, 1993) was used in the analyses. Large strains were accommodated in the computation by updating the nodal coordinates during the deformation process. More information on these sites and test procedures can be found in Byrne et al. (1995). The procedure involves fitting the model by varying K_{SP} manually until a reasonable match between the computed and observed material response is obtained. The remaining parameters were obtained from the guidelines provided in the preceding section. The results of the exercise is shown in Figure 3. The cavity strain, ϵ_θ, which is defined as the radial

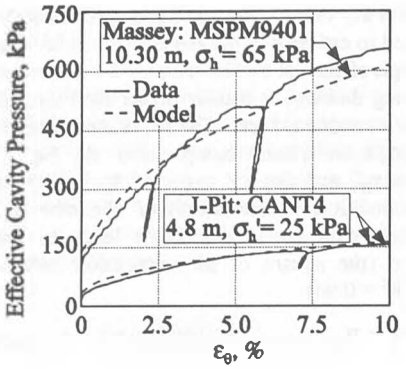

Figure 3. Simulation of SBPMT

deformation at the cavity wall divided by the original radius of the cavity, is plotted against the corresponding effective cavity pressure in the figure. The depth of SBPMTs are also indicated in the figure. Model parameters obtained from the inverse modeling are listed in Table 3. A Poisson's ratio of 0.2 was used and m_A was set equal to 2.0. Values of parameters C and p were 0.0006 and 0.9, respectively. Using the results, the undrained triaxial behavior of Syncrude tailings and Fraser River sand is estimated (shown as broken lines in Figure 4).

Table 3. Model Parameters from SBPMT

Site	K_E	λ	μ	η_{FI}	$\Delta\eta$	K_{SP}	R_F
J-Pit	450	0.85	0.29	0.69	0.05	150	0.93
Massey	720	0.77	0.39	0.52	0.01	240	0.92

Undisturbed samples were extracted via ground freezing from locations adjacent to the SBPMTs and triaxial compression and extension tests were conducted in the laboratory. Tests on samples with relative densities at consolidation, D_{RC}, similar to those pertaining to the SBPMTs are shown in Figure 4. The samples were anisotropically consolidated to $\sigma_{vc}'=2\sigma_{hc}'$. Subscripts "c", "h" and "v" are used to denote consolidation, vertical, and horizontal, respectively. Other details on these tests are summarized in Table 4. Except for the pore water pressure response in TXC for the sample from J-Pit, the performance of the proposed procedure for model calibration from inverse modeling of SBPMT appears to be reasonable. It may therefore be suggested that in an elaborate analysis of an earth structure, the mechanical behavior of the material over a wide strain range can be estimated from well conducted SBPMTs. The success of such an attempt however is expected to depend upon (a) whether the constitutive model is capable of simulating the observed material behavior, and (b) existence of a reasonable a-priori knowledge about the appropriate bounds of values of the model parameters.

5 CONCLUSIONS

A stress-strain model is proposed in this study for frictional materials with inherent anisotropy. A detailed guideline for the selection of appropriate values of a majority of model parameters is also provided. Necessary and sufficient data are seldom

Table 4. Particulars of Triaxial Tests

Site	Test No.	e_c	e_{MAX}/ e_{MIN}	σ_{vc}' kPa	Test
J-Pit	FS5C1B31	0.811	0.930/	44	TXE
	FS5C1B32	0.804	0.550	44	TXC
Massey	M94F6C7A	0.914	1.102/	124	TXE
	M94F6C5B	0.908	0.715	117	TXC

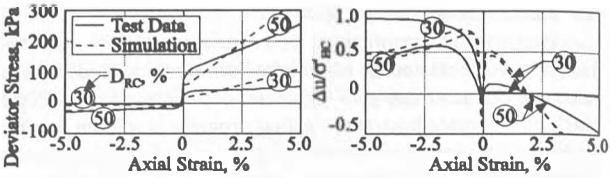

Figure 4. Predicted and observed triaxial behavior

available for calibration of a stress-strain model such as that described earlier. In such a situation, the constitutive model can be reasonably calibrated utilizing the guidelines and available test data. A procedure is suggested for calibrating the model from self-boring pressuremeter data. The procedure was validated by comparing the computed triaxial response with model parameters back figured from SBPMTs with the observed laboratory behavior of undisturbed samples. The proposed method based on inverse modeling of SBPMT can be useful in the assessment of static liquefaction potential; a problem in which the traditional empirical procedures based on in-situ tests such as SPT and CPTU have not been very successful.

ACKNOWLEDGEMENTS

This study was partly funded by the Canadian Liquefaction Experiment (CANLEX), Natural Sciences and Engineering Research Council of Canada (NSERC). The first author also would like to thank the University of British Columbia for financial support through University Graduate Fellowship.

REFERENCES

Been, K., and Jefferies M.G. 1985. A state parameter for sands: reply to discussion. *Géotechnique*, 35, 127-132.

Bolton, M.D. 1986. The strength and dilatancy of sands. *Géotechnique*, 36, 65-78.

Byrne P.M., Roy, D., Campanella, R.G., and Hughes, J. 1995. Predicting liquefaction response of granular soils from pressuremeter tests. Evans, M.D., and Fragaszy, R.J., Eds., Static and Dynamic Properties of Gravelly Soils, Geotechnical Special Publication No. 56, ASCE, 122-135.

Cundall, P.A. 1993. FLAC User's Manual, ITASCA Consulting Group, Inc., Minneapolis.

Lade, P.V. 1977. Elasto-plastic stress-strain theory for cohesionless soil with curved yield surfaces. *Int. J. of Solids and Structures*, London, 13, 1019-1035.

Lade, P.V., and Nelson, R.B. 1987. Modelling the elastic behaviour of granular materials. *Int. J. for Numerical and Analytical Methods in Geomechanics*, 11, 521-542.

Nakai, T., and Matsuoka, H. 1983. Shear behaviors of sand and clay under three-dimensional stress condition. *Soils and Foundations*, 23(2), 26-42.

Salgado, F.M. 1990. Analysis procedures for caisson-retained island type structures. *Ph.D. Dissertation*, Department of Civil Engineering, University of British Columbia, Vancouver.

Sasitharan, S., Robertson, P.K., Sego, D.C., and Morgenstern, N. R. 1994. State-boundary surface for very loose sand and its practical implications. *Canadian Geotech. J.*, 31, 321-334.

Srithar, T. 1994. Elasto-plastic deformation and flow analysis in oil sand masses. *Ph.D. Dissertation*, Department of Civil Engineering, University of British Columbia, Vancouver.

Stark, T.D., and Mesri, G. 1992. Undrained shear strength of liquefied sands for stability analysis. *J. of Geotech. Engrg.*, ASCE, 118, 1727-1747.